

An Exo-Jupiter Candidate in the Eclipsing Binary FL Lyr

V. S. Kozyreva¹, A. I. Bogomazov¹, B. P. Demkov^{2,3},
L. V. Zotov¹, A. V. Tutukov⁴

¹*Sternberg Astronomical Institute, Lomonosov Moscow State University,
Universitetskii pr. 13, Moscow, 119991 Russia*

²*“IT Project”, Savelkinskii proezd 4, Zelenograd, Moscow, 124482 Russia*

³*All-Russian Research Institute of Physical, Technical,
and Radio Technical Measurements,
Mendeleevo, Moscow Region, 141570 Russia*

⁴*Institute of Astronomy, Russian Academy of Sciences,
ul. Pyatnitskaya 48, Moscow, 119017 Russia*

Light curves of the eclipsing binary FL Lyr acquired by the Kepler space telescope are analyzed. Eclipse timing measurements for FL Lyr testify to the presence of a third body in the system. Preliminary estimates of its mass and orbital period are $\gtrsim 4M_J$ and $\gtrsim 7$ yrs. The times of primary minimum in the light curve of FL Lyr during the operation of the Kepler mission are presented.

1 INTRODUCTION

Extra-solar planetary systems remained hypothetical objects until the 1990s, when modern means for their detection were developed. Since then, some 10^4 candidate exoplanets have been discovered using various methods; the existence of many of these exoplanets has been reliably confirmed [1]. The vast majority of the discovered planets orbit single stars or individual components of wide multiple systems.

Currently, we know of eight exoplanets in five stellar systems and two candidate planets that simultaneously orbit both components of binaries, with both stars on the main sequence. The first planet discovered in such a binary was Kepler-16 (AB)b [2]. Others include Kepler-34 (AB)b and Kepler-35 (AB)b [3], Kepler-38 (AB)b [4], Kepler-47 (AB)b Kepler-47 (AB)c [5], PH1-Kepler-64 b [6], Kepler-413 (AB)b [7, 8], a possible third planet in the Kepler-47 [9] system and the candidate planet KIC 9632895 (AB)b [10]. Several planets near cataclysmic variables and a planet near the young star FW Tau [1] have also been discovered.

Searching for planets in binary systems is important for a number of reasons. Though it follows from [11] that planetary orbits in binaries exhibit long-term stability, it remains to be confirmed from observations that planets can survive in systems with various parameters. The systems known up to now have very similar parameters. The presence or absence of planets in binary systems and the systems' parameters are very important for our understanding of the processes of star and planet formation (e.g., [12]). In addition,

binary systems are more favorable for harboring life than single stars, and could in principle have several inhabited planets [13]. This makes searches for planets in various binary systems very important for searches for extraterrestrial, possibly even intelligent, life. A list of binary stars suitable for planetary searches can be found in [14], and includes the FL Lyr system.

In 2009-2014, the area of the sky containing FL Lyr was in the field of view of the Kepler space telescope [15], which was launched into near-solar orbit with the aim of searching for exoplanets. During these years, the telescope carried out a continuous photometric sky survey, during which a large amount of observing material was accumulated for FL Lyr. The Kepler observations can be used to study various scientific problems. In particular, a third body orbiting an eclipsing variable star gives rise to periodic shifts of the system’s center of mass with respect to the observer, causing the observed orbital period of the binary to vary about a certain value. The aim of our current study is to study the light-time effect in the FL Lyr system¹.

2 THE ECLIPSING BINARY FL Lyr

The eclipsing variable FL Lyr was discovered on photographic plates in 1935 [16]. Its minima are deep, with the change in the star’s brightness at the primary and secondary minimum being different by a factor of two: $m_{max} = 9^m.27$, $m_{min\ I} = 9^m.89$, $m_{min\ II} = 9^m.52$. According to the “General Catalog of Variable Stars” [17], $P_{orb} = 2.^d1781544$. The stars in the system have different sizes and spectral types. In the 1950s, Struve [18] obtained a spectroscopic radial-velocity curve of the primary and determined its spectral type to be G5.

In 1963, Cristaldi [19] obtained a photoelectric light curve and derived the photometric parameters of the system. He was able to estimate the masses of both components using earlier spectroscopy from various studies, both published and unpublished. The component parameters he found suggest that the two stars form an Algol-type system. In such systems, the primary (initially the higher-mass component) has left the main sequence (MS) and begun its expansion; in the process, the star has transferred some of its mass to the secondary. The mass of the primary becomes lower and its radius larger than its companion. At the same time, the primary is still on the MS, and the primary’s luminosity is lower than the secondary’s. This star is thus erroneously taken to be the secondary, while its companion, which initially had lower mass and is on the MS, is taken to be the primary.

Cristaldi [19] presents parameters calculated for the FL Lyr system: one of the components has a mass of $M_1 = 1M_\odot$, a relative radius² $r_1 = 0.132$ and a relative luminosity³ in the V filter $L_1 = 0.234$, while the second component has $M_2 = 1.1M_\odot$, $r_2 = 0.114$, $L_2 = 0.430$. This thus appears to be an Algol-type system, when the lower-mass star has a larger radius than the higher-mass one. A so-called “third light”, $L_3 = 0.336$, is also present in the solution, and belongs to either a field star or a third component in the system. The binary components move in a plane almost orthogonal to the plane of the sky;

¹In other words, to perform timing of the minima of the FL Lyr light curve.

²Expressed in fractions of the orbital semi-major axis of FL Lyr.

³Expressed in fractions of the system’s combined luminosity.

the estimated product of the eccentricity and longitude of periastron $e \cdot \cos\omega \leq 0.0002$. The orbits of the components are essentially circular. According to [19], the spectral types of the stars are estimated to be G0V + G5V.

In this study of the FL Lyr light curve, Botsula [20] found that the systems light decreased near the secondary minimum. She proposed that the system contained diffuse matter situated close to the secondary, which blocks some of the light in the secondary eclipse and distorts the shape of this part of the curve. This hypothesis is fully in accord with the physics of Algol-type stars, where the envelope of the more evolved primary flows toward the secondary. Moreover, the FL Lyr light curve displayed episodes of fading by as much as $0.^m04 - 0.^m05$. It is possible that all these distortions have a random character, due to systematic errors in the particular part of the FL Lyr light curve studied in [20].

In 1986, Popper et al.[21] obtained photoelectric light curves and spectroscopic radial-velocity curves of FL Lyr. They derived a new photometric solution of the light curve ($r_1 = 0.140$, $r_2 = 0.105$, $i = 86^\circ.3$, $L_1 = 0.79$, $L_2 = 0.21$), and estimated the stellar masses and spectral types: $1.22M_\odot$, $0.96M_\odot$, F8+G8. The binary orbit is circular with high accuracy. Comparing the observed parameters of the system to those determined from theoretical evolutionary tracks of stars of the same mass, they estimated the age of the FL Lyr system to be $5.3 \cdot 10^7 - 3.55 \cdot 10^9$ yrs, with the most likely age being $2.29 \cdot 10^9$ yrs [22]. Since the MS lifetime of a star with a mass of $1.2M_\odot$ is approximately $4.9 \cdot 10^9$ (Eq. 6 in [23]), neither component of FL Lyr has left the MS. No third light was detected in [21]. When calculating the photometric parameters, an upper limit $k \leq 1$ was imposed on the parameter $k = r_2/r_1$ (the ratio of the radii of the secondary and the primary). This excludes all solutions for which the two stars form an Algol-type system, i.e., a system with a reversed component-radius ratio. However, Popper et al. [21] suggest that the correctness of their derived parameters is supported by the lack of systematic deviations between the calculated and observed values for the brightness difference as a function of time. The parameters of the stars differ considerably from the solution found by Cristaldi [19]. Among the characteristic features of the light curves, Popper et al. [21] noted a brightness modulation ($\Delta m = 0.^m007$), which they attributed to the axial rotation of the components.

3 OBSERVATIONS OF FL Lyr WITH THE KEPLER SPACE TELESCOPE

We studied data obtained with Kepler. The main goal of the Kepler project was to search for exoplanets using observations of their transits. We used the Kepler data for eclipse-timing measurements (determining the light-time effect) for FL Lyr. Detailed information on the Kepler space telescope can be found in [24].

The Kepler data we used can be found in the Barbara A. Mikulski Archive for Space Telescopes [25], which is supported by the Space Telescope Science Institute. The identification number of FL Lyr in the Kepler Input Catalog is 9641031. Detailed information on the search and retrieval of data from the archive can be found in [24].

The Kepler archive consists of data files in FITS format. Two versions of these files are provided: LC (long cadence) and SC (short cadence). LC is the main version; these

data were collected once each 30 minutes. One LC FITS file contains observations of one object over one quarter⁴. SC (short cadence) SC is a complementary version of the data (intended for variability and asteroseismology studies); these data were collected once each minute. A single SC FITS file provides data for one month for a single object. Because of the design of Kepler, SC data were not accumulated during every quarter of the telescope’s operation. SC data for FL Lyr are fully available only for the observing quarters 7, 8, 13, 14, 15, and 16. To improve the accuracy of our study, we used the FITS files obtained in SC mode. We converted the FITS files to a form convenient for the analysis using the IRAF software with the PyRAF extension (the `kepconvert` routine, which converts FITS files to text files).

4 THE LIGHT-TIME EFFECT IN FL Lyr

One of the methods that can be used to detect a third body in an eclipsing system is to search for the light-time effect. The periods of the primary and secondary minima will oscillate if the distance between the center of the solar system and the center of the eclipsing system varies. Any third body in a binary system makes the system’s center of mass move with the period of this body’s orbit⁵. The comparatively short period of the stars’ orbit about the common center (about two days) makes it possible to identify a large number of light curves within minima in the Kepler observations. Our aim is to look for the light-time effect in the FL Lyr system; i.e., to search for shifts in the observed times of minima relative to the calculated values.

The orbit of a binary system rotates due to tidal forces between the two stars and general relativistic effects. In the case of an elliptical orbit, this rotation is manifest through apsidal motion, which gives rise to a shift of the observed relative to the calculated times of minima. For FL Lyr, with its practically circular binary orbit ($e \leq 0.0002$), theoretical estimates of the apsidal motion predict the period of this motion to be longer than 100 years, and its amplitude to be below 10 s. This effect is very small over the time interval of the Kepler observations, can be neglected. We are looking for the light-time effect with much shorter periods.

We considered solely the primary minima. These are symmetric and deep ($\approx 0.^m6$) – more than twice as deep as the secondary minima – increasing the accuracy of the timing of the minima by the same factor. We identified 600 Kepler light curves within primary minima of FL Lyr.

Kepler observations possess systematic errors (see, for instance, section 7.1 in [24]) – so-called linear trends, which can reach several hundredths of a magnitude during the duration of a minimum in the FL Lyr light curve. Our study of the FL Lyr light curves already corrected for this linear trend using correction factors shows that the trend was

⁴The light curves within the FL Lyr minima contain only five to six data points in the LC mode.

⁵The stability of planetary orbits in binary systems was studied in [11]; according to Table 6 in [11], the orbit of a planet around the central binary will be stable if the semi-major axis of the planet’s orbit is approximately a factor of four or more larger than the semi-major axis of the binary orbit; i.e., if the orbital period of the planet is longer than the orbital period of the central binary star by a factor of 10 or more, as follows from Kepler’s third law. Thus, the conditions for the long-term survival of planets in the FL Lyr system are satisfied for planetary orbital periods exceeding 20 days.

not fully removed, so that the shape of the light curves during minima remains distorted. The brightness difference between the ingress and egress reaches several ten-thousandths of a magnitude, with different signs for different light curves. Distortions by one ten-thousandth of a magnitude for the primary minima of FL Lyr translate into an error of approximately 2 s in the times of minima. This is a large error, and is able to completely distort the light-time effect due to the presence of a planet with an amplitude of the order of 5-6 s.

Light-time effects for 1279 close eclipsing binary systems were studied by Conroy et al. [26], who report the discovery of 236 eclipsing binaries with suspected third bodies. This study will be supplemented with an analysis of orbital-period variations (Orosz et al., in preparation; see [26]). It will be very interesting to compare our results to those of Orosz et al.

We studied individual light curves of primary minima of FL Lyr obtained with Kepler and calculated individual correction factors to remove the linear trend in each case, based on the hypothesis that the brightnesses at the eclipse ingress and egress are intrinsically the same. Since changes in the trend correction factors occur only rarely, no more than twice during the period of FL Lyr, we adopted the hypothesis that the trend does not change significantly within a light-curve minimum (≈ 4 hours), and corrected the light curve using a single set of correction coefficients that were specific to each minimum. Even if the origins of the different brightnesses at the beginnings and ends of minima are physical, our approach enables us to search for the light-time effect, since we are studying the dynamics of changes in the times of minima. If the light curve changes slowly compared to the observing period, all the times of minima will be displaced relative to the true times, but the magnitude of this shift will not influence the amplitude of the light-time effect. If, however, the changes in the light curve are comparable to the duration of the observations, which is very improbable, the light-time effect will be determined with additional systematic errors. Nevertheless, the period of the light-time effect can be derived from the light curve. When determining the times of the primary minima, we used a template theoretical light curve calculated from the orbital elements and the relative parameters of the stars in this binary system.

When calculating the photometric elements, we used the combined light curves compiled from observations obtained in the SC mode; these contained only neighboring observations within primary and secondary minima (Fig. 1 shows a sample light curve of FL Lyr). The photoelectric light curves of FL Lyr obtained by Popper et al. [21] exhibit the same out-of-eclipse brightness level for both minima. We used this finding when selecting light curves used to calculate the photometric elements. Since the observations are distorted by the linear trend, we tried to select light curves for which this was minimal. The influence of the trend in each case is a random value, and the resulting sets of elements had nearly normal distributions. The parameter most important in the search for the light-time effect is the shift of the observed times of primary minimum relative to the calculated times (O-C). These shifts depended only weakly on variations of the other parameters we determined, presented in Table 1. Column 2 of this table contains the ranges of the parameters found for the various light curves of FL Lyr. Column 3 gives the set of parameters we used to derive the theoretical curve we then applied as a template.

The CCD chip of the spacecraft has a broad filter ranging from 430 to 890 nm, corre-

sponding to the combined range of the B, V, and R filters of the Johnson photometric system. Therefore, it is not correct to compare photometric elements based on these light curves with elements derived using light curves obtained in the Johnson filters; this is especially true for the luminosities of the components.

We used a quasi-Newtonian method with analytical computation of the functional derivatives as a minimization algorithm⁶. The minimization functional contains the sum of the squared differences between the observed and theoretical magnitudes at each point, including simple and linear limitations for the parameter values we seek. Because of their very weak influence on the light curves, we did not vary the limb-darkening coefficients u_1 and u_2 , and fixed them in accordance with the spectral types of the binary components (F8V + G8V [21]). Values for the theoretical coefficients u_1 and u_2 corresponding to wavelengths in the middle of the instrumental range were taken from [32]. Some of the parameters we determined in our free search for the orbital elements and parameters differ considerably from those obtained by Popper [21]; this is especially true for component luminosities. This can partially be explained by the different spectral ranges used. In our current study, we are interested in the set of elements only as a tool for deriving a theoretical curve that most closely approaches the observed curves at the primary minima.

Times of minima we collected from the literature are presented in Fig. 2 and Table 2. The scatter of the data points in Fig. ± 15 minutes. The scatter of the photoelectric times of minima can reach ± 1.5 minutes. This large scatter of the times of minima can be explained in many ways, some of them described above. Our aim was to find the amplitude of the light-time effect with an accuracy of seconds. The large scatter in the previously published times of minima makes those data unsuitable for this. Accordingly, we used only the long uniform series of Kepler observations, deriving the times of minima using the same algorithm.

We used only data points corresponding to primary minima of FL Lyr (phases from 0.94 to 1.06). After obtaining the light curve for an individual minimum without the linear trend, we then calculated the shift of the observed time of minimum from the calculated time. We applied an algorithm for calculating the minimal deviation between the observed and theoretical light curves⁷; the only free parameter was the shift of the primary minimum, with all other parameters being fixed at the values indicated in column 3 of Table 1. The criterion for our solution was a symmetric position of the deviations (between the observed and calculated light-curve points) relative to zero phase. We checked this by determining the linear trend in the O-C residuals, with the result being considered satisfactory only in the absence of any trend. This procedure was performed for all primary minima of FL Lyr observed with Kepler; the times of minima are collected in the first column of 3, while the second column contains the O-C residuals: the differences between the observed times of minima and the theoretical times of minima calculated with the ephemeris (1).

Searching for the light-time effect requires as accurate as possible knowledge of the binary's orbital period, on which the parameters of the light-time effect depend. We used three values of the orbital period of FL Lyr. The period $P_{10} = 2.17815440^d$ was taken

⁶The same algorithm was used earlier in [27]–[31], resulting in the discoveries of brown dwarfs in the HP Aur and AS Cam systems.

⁷ See [27]–[31] for details.

from [19] (this is also the period given in [17]). The period $P_{11} = 2^d.17815408^d$ data. Finally, the orbital period $P_{13} = 2^d.17815414$ was calculated using all the ground-based observations and six Kepler times of minima⁸. The system ephemerides for these three periods are

$$\text{Min } I(HJD) = 2438221.55250 + 2.17815440 \times E; \quad (1)$$

$$\text{Min } I(HJD) = 2438221.55239 + 2.17815408 \times E; \quad (2)$$

$$\text{Min } I(HJD) = 2438221.55211 + 2.17815414 \times E; \quad (3)$$

The gray triangles in Fig. 2 are the O-C values calculated with the ephemeris (1) for the times of minima from the literature; the black circles are our values calculated using the Kepler observations. The shift in the times of minima we are seeking is clearly visible.

We carried out our further analysis of the data obtained for the three periods (P_{10} , P_{11} , P_{12}). The large scatter of the O-C deviations limits our ability to obtain many parameters of the light-time effect. To minimize the number of parameters, we adopted the simple hypothesis that the third body undergoes circular motion about the eclipsing binary. Using a Fourier expansion⁹, we analyzed the O-C residuals obtained for each of the periods and the calculated parameters of the best-fit sine curve approximating the time dependence of the times of minima (the light-time effect). Table 4 presents the amplitudes and periods of this theoretical curve. Figure 3 presents the power spectrum for the O-C residuals calculated using the ephemeris 1, and Fig. 4 displays a part of 3 on a larger scale. The peak near a period of ≈ 2 days corresponds to the orbital period of FL Lyr; this is clearly visible in Fig. 5. A peak at about 5-6 yrs is also visible in Fig. 3; this is due to the light-time effect. It is difficult to search for a larger number of objects in the system due to the large scatter of the available times of minima, comparable to the amplitude of the light-time effect. The O-C calculations performed for all three periods (P_{10} , P_{11} , P_{12}) demonstrate systematic deviations that can be explained as a light-time effect with a period somewhat larger than the entire time interval covered by the Kepler observations. Figures 6, 7 and 8 show the O-C deviations of the times of minima as a function of the orbital phase of the third body.

If less than a half of the period of the light-time effect elapsed during the time covered by the Kepler observations, an alternative explanation for the observed systematic shifts could be a variation of the close-binary period ($dP \sim 10^{-5}$ days/year). The system has already been observed for a long time, and period variations of this kind should already have been detected from the parabolic shape of the O-C curve. During the time interval of the observations (almost 60 years), the FL Lyr period variations would have already accumulated in the fourth place after the decimal point, and the period should be increasing, while all the previously measured period values [34]-[50] are not lower than

⁸So that the space data would not dominate the other measurements, we took three Kepler times of minima for 2009 and three for 2014. The 2009 times of minima are HJD-2400000 = 54965.02424, 54967.20240, and 54969.38054, and the 2014 times are HJD-2400000 = 56385.18082, 56387.35900, and 56389.53716.

⁹We applied the PERDET (PERiod DETermination) code [33].

those we have derived. This can be taken as evidence against the hypothesis that the system’s period is varying, and that the times of minima exhibit variations due to the light-time effect.

5 MASS OF THE THIRD BODY

In the general case, accurately determining the mass of a body in a binary, and especially a multiple, system can require a dedicated, complex study. There is no sense in carrying out such estimates in the framework of our current study, since the orbital period of the third body has not been accurately determined, and is longer than the time covered by the Kepler observations. Moreover, we were not able to derive the orbital inclination of the third body relative to the orbital plane of the system. Therefore, we have obtained a simple lower limit for the third body’s mass.

Since the orbital period of the third body is much longer than the orbital period of the central binary, we can use Kepler’s third law to obtain a simple mass estimate¹⁰

$$P_{orb} = 0.1 \frac{a^{3/2}}{M^{1/2}}, \quad (4)$$

where P_{orb} is the orbital period of the third body in days, a the semi-major axis of the third body’s orbit in solar radii, and M the combined mass of the two components of FL Lyr and the third body in solar masses.

The sum of the component masses in the FL Lyr system is $\approx 2M_{\odot}$ [21]. The orbital period of the third body with the ephemeris 1 is $\gtrsim 7$ years. According to 4, the semi-major axis of the orbit of the third body is $\gtrsim 1100R_{\odot}$. The amplitude of the light-time effect with the same ephemeris is 4.8 s. During this time, light traverses half the distance of the periodic shift of the FL Lyr binary due to the third body; i.e., the semi-major axis of the orbit of the FL Lyr system about the center of mass of the FL Lyr-third body system is approximately $2R_{\odot}$. Thus, the ratio of the third body’s mass to the mass of the FL Lyr binary is $\approx 1/500$. We thus get the simple estimate for the third body’s mass $2M_{\odot}/500 \approx 4M_J$. If the orbital period of the third body proves to be longer than our estimate, the estimated mass of this body will be lower; at the same time, the orbital inclination of the third body will increase its estimated mass. Note that the orbital planes for all eight known exoplanets in orbits around binaries are very close (within 1°) to the orbital planes of their parent binaries. Thus, our rough estimate of the planet’s mass may prove to be close to the actual mass of this planet.

6 CONCLUSIONS

We have analyzed Kepler light curves for the eclipsing binary FL Lyr and detected the light-time effect, indicating that the system probably contains a body with a mass of about four Jupiter masses, with an orbital period around the close binary of ≥ 7 yrs.

¹⁰The orbital period of the third body is 7 years or more, compared to the 2-day orbital period of FL Lyr; stable orbits admitting application of Kepler’s third law (for rough estimates, since there will definitely be perturbations of the third body’s orbit) would begin with an orbital period of 20 days [11].

Confirmation of this planet’s existence will require long-term photometric observations of FL Lyr with an accuracy no worse than that of the Kepler data; otherwise, it will be necessary to analyze the radial-velocity curve of the system over a long time and with very high accuracy.

The times of minima we have derived from the light curve of FL Lyr (Table 3) can be used in further studies of the system.

Discoveries of planets in close binary systems in recent years mean that the formation of two stellar components during the collapse of a rotating protostellar cloud does not completely resolve the problem of the inevitable angular-momentum excess in protostellar clouds. The formation of planets in circum- stellar accretion-decretion disks remains necessary to completely resolve this problem. As a result, the components of wide, as well as close, binary systems could have planets around them. This means that most stars can possess planetary systems, so that the formation rate of planetary systems could be close to the star-formation rate (see, for instance, the recent paper [51]). This rate for the Milky Way would thus be several planetary systems per year.

7 ACKNOWLEDGEMENTS

The authors thank A.I. Zakharov, S.E. Leontyev, and V.N. Sementsov, who developed software for the computation of photometric elements of eclipsing binaries.

References

1. exoplanet.eu.
2. L. R. Doyle, J. A. Carter, D. C. Fabrycky, et al., *Science* **333**, 1602 (2011).
3. W. F. Welsh, J. A. Orosz, J. A. Carter et al., *Nature* **481**, 475 (2012).
4. J. A. Orosz, W. F. Welsh, J. A. Carter et al., *Astrophys. J.* **758**, 14 (2012).
5. J. A. Orosz, W. F. Welsh, J. A. Carter et al., *Science* **337**, 1511 (2012).
6. M. E. Schwamb, J. A. Orosz, J. A. Carter et al., *Astrophys. J.* **768**, 21 (2013).
7. V. B. Kostov, P. R. McCullough, J. A. Carter et al., *Astrophys. J.* **784**, 18 (2014).
8. V. B. Kostov, P. R. McCullough, J. A. Carter et al., *Astrophys. J.* **787**, 1 (2014).
9. N. C. Hinse, N. Haghighipour, V. B. Kostov, K. Gozdziewski, eprint arXiv:1409.1349.
10. W. F. Welsh, J. A. Orosz, D. R. Short et al., arXiv:1409.1605.
11. M. J. Holman, P. A. Wiegert, *Astronomical Journal* **117**, 621 (1999).
12. A. V. Tutukov and A. V. Fedorova, *Astron. Rep.* **56**, 305 (2012).
13. P. A. Mason, J. I. Zuluaga, J. M. Clark et al., *Astrophysical Journal Letters* **774**, L26, 8 (2013).

14. A. V. Tutukov and A. I. Bogomazov, *Astron. Rep.* **56**, 775 (2012).
15. The Kepler Field Of View <http://keplergo.arc.nasa.gov/CalibrationFOV.shtml>.
16. O. Morgenroth, *Astronomische Nachrichten* **255**, 425 (1935).
17. N. N. Samus, O. V. Durlevich, E. V. Kazarovets, et al., General Catalog of Variable Stars (GCVS database) CDS B/gcvs.
18. O. Struve, H. G. Horak, R. Canavaggia et al., *Astrophysical Journal* **111**, 658 (1950).
19. S. Cristaldi, *Memorie della Societa Astronomia Italiana* **36**, 77 (1965).
20. R. A. Botsula, *Perem. Zvezdy* **20**, 588 (1978).
21. D. M. Popper, C. H. Lacy, M. L. Frueh, A. E. Turner, *Astronomical Journal* **91**, 383 (1986).
22. E. Lastennet, D. Valls-Gabaud, *Astron. Astrophys.* **396**, 551 (2002).
23. V. M. Lipunov, K. A. Postnov, M. E. Prokhorov, and A. I. Bogomazov, *Astron. Rep.* **53**, 915 (2009).
24. Kepler Archive Manual <https://archive.stsci.edu/kepler/documents.html> Kepler Data Characteristics Handbook.
25. Kepler Archive <https://archive.stsci.edu/kepler/>.
26. K. E. Conroy, A. Prsa, K. G. Stassun et al., *Astronomical Journal* **147**, 14 (2014).
27. Kh. F. Khaliullin, V. S. Kozyreva, *Astrophys. and Space Science* **94**, 115 (1983).
28. V. S. Kozyreva, *Astrophys. and Space Science* **165**, 1 (1990).
29. V. S. Kozyreva and A. I. Zakharov, *Astron. Lett.* **27**, 712 (2001).
30. V. S. Kozyreva, A. V. Kusakin, and Kh. F. Khaliullin, *Astron. Lett.* **31**, 117 (2005).
31. V. S. Kozyreva and A. I. Zakharov, *Astron. Lett.* **32**, 313 (2006).
32. W. van Hamme, *Astronomical Journal* **106**, 2096 (1993).
33. M. Breger, *Delta Scuti Star Newsletter*, 21 (1990).
34. L. J. Robinson, *Information Bulletin on Variable Stars* **111** (1965).
35. A. D. Mallama, *Astrophys. J. Suppl. Ser.* **44**, 241-272 (1980).
36. C. D. Scarfe, D. W. Forbes, P. A. Delaney, J. Gagne, *Information Bulletin on Variable Stars* **2545** (1984).
37. V. Keskin, E. Pohl, *Information Bulletin on Variable Stars* **3355** (1989).

- 38. J. Safar, M. Zejda, Information Bulletin on Variable Stars **4887** (2000).
- 39. H. J. Deeg, L. R. Doyle, B. J. S. Bejar, et al., Information Bulletin on Variable Stars **5470** (2003).
- 40. F. Agerer, J. Hubscher, Information Bulletin on Variable Stars **4912** (2000).
- 41. R. Nelson, Information Bulletin on Variable Stars **4840** (2000).
- 42. F. Agerer, J. Hubscher, Information Bulletin on Variable Stars **5484** (2003).
- 43. C.-H. Kim, C.-U. Lee, Y.-N. Yoon, et al., Information Bulletin on Variable Stars **5694** (2006).
- 44. J. Hübscher, A. Paschke, F. Walter, Information Bulletin on Variable Stars **5657** (2005).
- 45. J. M. Cook, M. Divoky, A. Hofstrand, et al., Information Bulletin on Variable Stars **5636** (2005).
- 46. J. Hübscher, A. Paschke, F. Walter, Information Bulletin on Variable Stars **5731** (2006).
- 47. M. Zejda, Z. Mikulasek, M. Wolf, Information Bulletin on Variable Stars **5741** (2006).
- 48. J. Hübscher, H.-M. Steinbach, F. Walter, Information Bulletin on Variable Stars **5889** (2009).
- 49. G. Samolyk, The Journal of the American Association of Variable Star Observers **36**, 186 (2008).
- 50. G. Samolyk, The Journal of the American Association of Variable Star Observers **39**, 94 (2011).
- 51. S. Ballard, J. A. Johnson, eprint arXiv:1410.4192.

Table 1: Parameters derived from the Kepler light curves and adopted in the calculations of the theoretical light curve of FL Lyr r_1 , r_2 are the radii of the primary and the secondary in units of the semi-major axis of FL Lyr; e the orbital eccentricity; ω the longitude of periastron; L_1 , L_2 the luminosities of the primary and secondary in units of the systems luminosity; L_3 the “third light” in units of the system’s luminosity; u_1 , u_2 limb-darkening coefficients for the primary and secondary; and σ the standard (O-C) deviation. (O-C).

Parameters	Value for FL Lyr	Values adopted in the computations
r_1	0.122-0.133	0.123
r_2	0.118- 0.126	0.123
i	$85^\circ.3 - 86^\circ.5$	$85^\circ.9$
e	0-0.0002	0
ω	0-360°	0
L_1	0.520-0.610	0.596
L_2	0.260-0.310	0.298
L_3	0.008-0.22	0.106
u_1	0.62 (fixed)	0.62 (fixed)
u_2	0.68 (fixed)	0.68 (fixed)
σ_{O-C}	-	$0.^m00026$

Table 2: Times of primary minima of FL Lyr from ground- based observations, the O-C deviations were calculated using the ephemeris 1.

Time of primary minimum, HJD-2400000	(O-C), days	Reference
38173.6400	0.00690	[34]
38221.5525	0.00000	[19]
40038.1368	0.00350	[35]
40770.0011	0.00800	[35]
41133.7419	-0.00303	[35]
41499.6666	-0.00830	[35]
41865.6053	0.00050	[35]
42229.3473	-0.00930	[35]
42595.2820	-0.00454	[35]
42961.2145	-0.00197	[35]
43690.8989	0.00070	[35]
44459.7830	-0.00370	[36]
45572.8218	-0.00180	[36]
46925.4551	-0.00238	[37]
49909.5271	-0.00191	[38]
50654.4547	-0.00312	[39]
51266.5174	-0.00180	[40]
51440.7700	-0.00155	[41]
52806.4725	-0.00186	[42]
52911.0235	-0.00227	[43]
53209.4302	-0.00273	[44]
53531.7977	-0.00208	[45]
53555.7555	-0.00400	[45]
53612.3871	-0.00439	[46]
53673.3777	-0.00211	[46]
53684.2691	-0.00149	[47]
54466.2261	-0.00192	[48]
54583.8446	-0.00375	[49]
54594.7376	-0.00152	[49]
54642.6572	-0.00132	[49]
55304.8135	-0.00396	[50]
55437.6827	-0.00218	[50]

Table 3: Times of primary minima of FL Lyr found from Kepler data, the O-C deviations were calculated using the ephemeris 1.

Moment, HJD-2400000	(O-C), days
54965.02424	-0.00113
54967.20240	-0.00113
54969.38054	-0.00114
54971.55866	-0.00118
54973.73682	-0.00117
54975.91499	-0.00115
54978.09314	-0.00116
54980.27127	-0.00118
54982.44946	-0.00115
54984.62759	-0.00117
54986.80578	-0.00114
54988.98393	-0.00114
54991.16210	-0.00113
54993.34026	-0.00112
54995.51841	-0.00112
54997.69669	-0.00100
55004.23105	-0.00110
55006.40922	-0.00109
55008.58736	-0.00110
55010.76549	-0.00113
55012.94365	-0.00112
55017.29999	-0.00109
55019.47812	-0.00111
55021.65625	-0.00114
55023.83439	-0.00115
55026.01257	-0.00113
55028.19073	-0.00112
55030.36885	-0.00115
55032.54697	-0.00119
55034.72509	-0.00122
55036.90328	-0.00119
55039.08140	-0.00122
55041.25957	-0.00121
55043.43771	-0.00122
55045.61584	-0.00125
55047.79406	-0.00118
55049.97218	-0.00121
55052.15043	-0.00112
55054.32850	-0.00120
continuation in the next page	

Table 3 – continuation

Moment, HJD-2400000	(O-C), days
55056.50666	-0.00120
55060.86302	-0.00115
55063.04122	-0.00110
55065.21935	-0.00113
55067.39750	-0.00113
55069.57563	-0.00115
55071.75385	-0.00109
55073.93203	-0.00106
55076.11020	-0.00105
55078.28829	-0.00111
55080.46645	-0.00111
55082.64459	-0.00112
55084.82276	-0.00110
55087.00089	-0.00113
55091.35710	-0.00123
55093.53539	-0.00109
55095.71356	-0.00108
55097.89167	-0.00112
55100.06984	-0.00111
55102.24797	-0.00113
55104.42610	-0.00115
55106.60426	-0.00115
55108.78242	-0.00114
55110.96060	-0.00112
55113.13873	-0.00114
55115.31692	-0.00111
55117.49504	-0.00114
55119.67321	-0.00113
55121.85135	-0.00114
55124.02950	-0.00114
55126.20765	-0.00115
55128.38578	-0.00117
55132.74208	-0.00118
55134.92022	-0.00120
55137.09838	-0.00119
55139.27653	-0.00119
55141.45468	-0.00120
55143.63282	-0.00121
55145.81099	-0.00120
55147.98918	-0.00116
55150.16731	-0.00119
55152.34548	-0.00117
continuation in the next page	

Table 3 – continuation

Moment, HJD-2400000	(O-C), days
55156.70175	-0.00121
55158.87990	-0.00121
55161.05809	-0.00118
55163.23632	-0.00110
55165.41448	-0.00110
55167.59263	-0.00110
55169.77094	-0.00095
55171.94888	-0.00116
55174.12705	-0.00115
55176.30523	-0.00112
55178.48340	-0.00110
55180.66164	-0.00102
55187.19601	-0.00111
55189.37422	-0.00106
55191.55238	-0.00105
55193.73047	-0.00111
55195.90868	-0.00106
55198.08687	-0.00102
55200.26502	-0.00103
55202.44317	-0.00103
55204.62133	-0.00103
55206.79947	-0.00104
55208.97767	-0.00100
55211.15577	-0.00105
55213.33390	-0.00107
55215.51200	-0.00113
55217.69013	-0.00115
55219.86829	-0.00115
55222.04642	-0.00117
55224.22459	-0.00116
55228.58090	-0.00116
55235.11540	-0.00112
55237.29356	-0.00111
55239.47174	-0.00109
55243.82801	-0.00113
55246.00621	-0.00108
55248.18439	-0.00105
55250.36247	-0.00113
55252.54061	-0.00114
55254.71876	-0.00115
55256.89700	-0.00106
55259.07514	-0.00108
continuation in the next page	

Table 3 – continuation

Moment, HJD-2400000	(O-C), days
55261.25326	-0.00111
55263.43145	-0.00108
55265.60958	-0.00110
55267.78771	-0.00112
55269.96587	-0.00112
55272.14398	-0.00116
55274.32208	-0.00122
55278.67836	-0.00125
55280.85650	-0.00126
55283.03465	-0.00127
55285.21281	-0.00126
55287.39099	-0.00123
55289.56916	-0.00122
55291.74733	-0.00120
55293.92549	-0.00120
55296.10362	-0.00122
55298.28180	-0.00120
55300.45997	-0.00118
55302.63812	-0.00118
55304.81631	-0.00115
55306.99439	-0.00122
55311.35074	-0.00118
55313.52889	-0.00119
55315.70703	-0.00120
55317.88525	-0.00114
55320.06334	-0.00120
55322.24152	-0.00117
55324.41968	-0.00117
55326.59804	-0.00096
55328.77600	-0.00116
55330.95426	-0.00105
55335.31062	-0.00100
55337.48874	-0.00104
55339.66684	-0.00109
55344.02316	-0.00108
55346.20128	-0.00111
55348.37940	-0.00115
55350.55753	-0.00117
55352.73568	-0.00118
55354.91386	-0.00115
55357.09203	-0.00113
55359.27017	-0.00115
continuation in the next page	

Table 3 – continuation

Moment, HJD-2400000	(O-C), days
55361.44831	-0.00116
55363.62648	-0.00115
55365.80460	-0.00118
55367.98278	-0.00116
55372.33909	-0.00116
55374.51723	-0.00117
55376.69534	-0.00121
55378.87356	-0.00115
55381.05167	-0.00119
55383.22987	-0.00115
55385.40802	-0.00115
55387.58616	-0.00117
55389.76436	-0.00112
55391.94264	-0.00100
55394.12078	-0.00101
55396.29897	-0.00097
55398.47699	-0.00111
55400.65524	-0.00101
55402.83331	-0.00110
55405.01151	-0.00105
55407.18966	-0.00106
55409.36777	-0.00110
55411.54600	-0.00102
55413.72416	-0.00102
55415.90226	-0.00107
55418.08049	-0.00100
55420.25857	-0.00107
55422.43676	-0.00104
55424.61487	-0.00108
55428.97120	-0.00106
55431.14933	-0.00108
55433.32744	-0.00113
55435.50560	-0.00112
55437.68373	-0.00115
55439.86184	-0.00119
55442.04001	-0.00118
55444.21819	-0.00115
55446.39635	-0.00115
55448.57448	-0.00117
55450.75262	-0.00118
55452.93078	-0.00118
55455.10892	-0.00119
continuation in the next page	

Table 3 – continuation

Moment, HJD-2400000	(O-C), days
55457.28713	-0.00114
55459.46531	-0.00111
55461.64348	-0.00110
55463.82164	-0.00109
55465.99978	-0.00110
55468.17791	-0.00113
55470.35605	-0.00114
55472.53419	-0.00116
55474.71229	-0.00121
55476.89043	-0.00123
55479.06858	-0.00123
55481.24671	-0.00126
55483.42489	-0.00123
55485.60302	-0.00125
55487.78119	-0.00124
55489.95944	-0.00114
55494.31569	-0.00120
55496.49389	-0.00116
55498.67206	-0.00114
55500.85025	-0.00111
55503.02841	-0.00110
55505.20660	-0.00106
55507.38474	-0.00108
55509.56290	-0.00107
55511.74103	-0.00110
55513.91917	-0.00111
55516.09734	-0.00110
55518.27549	-0.00110
55520.45362	-0.00112
55522.63181	-0.00109
55524.80995	-0.00110
55526.98808	-0.00113
55529.16624	-0.00112
55531.34442	-0.00110
55533.52251	-0.00116
55535.70065	-0.00118
55537.87880	-0.00118
55540.05696	-0.00117
55542.23514	-0.00115
55546.59147	-0.00113
55548.76963	-0.00112
55550.94781	-0.00110
continuation in the next page	

Table 3 – continuation

Moment, HJD-2400000	(O-C), days
55570.55110	-0.00120
55572.72927	-0.00118
55574.90746	-0.00114
55577.08559	-0.00117
55579.26373	-0.00118
55581.44194	-0.00113
55583.62010	-0.00112
55585.79823	-0.00115
55587.97637	-0.00116
55590.15452	-0.00117
55592.33267	-0.00117
55598.86711	-0.00119
55601.04526	-0.00120
55603.22343	-0.00118
55605.40162	-0.00115
55607.57978	-0.00114
55609.75796	-0.00112
55611.93609	-0.00114
55614.11423	-0.00115
55616.29246	-0.00108
55618.47067	-0.00102
55620.64884	-0.00101
55622.82710	-0.00090
55625.00513	-0.00103
55627.18320	-0.00111
55629.36134	-0.00112
55631.53942	-0.00120
55633.71776	-0.00101
55642.43022	-0.00117
55644.60847	-0.00108
55646.78657	-0.00113
55648.96475	-0.00110
55651.14298	-0.00103
55653.32105	-0.00111
55655.49912	-0.00120
55657.67740	-0.00107
55659.85545	-0.00118
55662.03376	-0.00102
55664.21186	-0.00108
55666.39007	-0.00102
55668.56813	-0.00111
55670.74631	-0.00109
continuation in the next page	

Table 3 – continuation

Moment, HJD-2400000	(O-C), days
55672.92436	-0.00119
55677.28069	-0.00117
55679.45889	-0.00113
55681.63700	-0.00117
55683.81515	-0.00117
55685.99329	-0.00119
55688.17145	-0.00118
55690.34958	-0.00121
55692.52779	-0.00115
55694.70594	-0.00116
55696.88411	-0.00114
55699.06225	-0.00116
55701.24044	-0.00112
55703.41853	-0.00118
55705.59667	-0.00120
55707.77467	-0.00135
55709.95298	-0.00120
55712.13117	-0.00116
55714.30934	-0.00115
55716.48749	-0.00115
55718.66564	-0.00116
55720.84373	-0.00122
55723.02189	-0.00121
55727.37829	-0.00112
55729.55646	-0.00111
55731.73468	-0.00104
55733.91276	-0.00112
55738.26903	-0.00115
55740.44726	-0.00108
55742.62547	-0.00102
55744.80362	-0.00103
55746.98179	-0.00101
55749.15991	-0.00105
55751.33807	-0.00104
55753.51623	-0.00104
55755.69433	-0.00109
55757.87245	-0.00112
55760.05061	-0.00112
55762.22869	-0.00119
55764.40680	-0.00124
55766.58501	-0.00118
55768.76315	-0.00120
continuation in the next page	

Table 3 – continuation

Moment, HJD-2400000	(O-C), days
55770.94133	-0.00117
55773.11953	-0.00113
55775.29767	-0.00114
55777.47579	-0.00117
55779.65396	-0.00116
55781.83212	-0.00115
55784.01024	-0.00119
55786.18851	-0.00107
55788.36667	-0.00107
55790.54489	-0.00100
55792.72297	-0.00107
55794.90112	-0.00108
55797.07925	-0.00110
55799.25740	-0.00111
55801.43556	-0.00110
55803.61371	-0.00111
55805.79183	-0.00114
55807.96999	-0.00114
55810.14815	-0.00113
55812.32630	-0.00113
55814.50448	-0.00111
55816.68261	-0.00113
55818.86073	-0.00117
55821.03886	-0.00119
55823.21710	-0.00111
55825.39518	-0.00118
55827.57334	-0.00118
55829.75152	-0.00115
55831.92960	-0.00122
55836.28598	-0.00115
55838.46413	-0.00116
55840.64225	-0.00119
55842.82045	-0.00115
55844.99861	-0.00114
55847.17675	-0.00115
55849.35494	-0.00112
55851.53301	-0.00120
55853.71115	-0.00122
55855.88933	-0.00119
55858.06744	-0.00124
55860.24565	-0.00118
55862.42379	-0.00120
continuation in the next page	

Table 3 – continuation

Moment, HJD-2400000	(O-C), days
55864.60193	-0.00121
55866.78009	-0.00120
55868.95822	-0.00123
55871.13645	-0.00115
55873.31456	-0.00120
55875.49279	-0.00112
55877.67097	-0.00110
55879.84907	-0.00115
55882.02721	-0.00117
55884.20530	-0.00123
55886.38349	-0.00119
55888.56164	-0.00120
55890.73973	-0.00126
55892.91789	-0.00126
55895.09595	-0.00135
55897.27421	-0.00125
55899.45237	-0.00124
55901.63047	-0.00129
55905.98673	-0.00134
55908.16495	-0.00128
55910.34310	-0.00128
55912.52125	-0.00129
55914.69954	-0.00115
55916.87759	-0.00126
55919.05580	-0.00120
55921.23397	-0.00118
55923.41208	-0.00123
55925.59032	-0.00114
55927.76846	-0.00116
55929.94663	-0.00114
55934.30273	-0.00135
55936.48115	-0.00109
55938.65905	-0.00134
55940.83741	-0.00113
55943.01557	-0.00113
55945.19372	-0.00113
55947.37191	-0.00110
55949.55006	-0.00110
55951.72812	-0.00120
55953.90642	-0.00105
55956.08457	-0.00105
55958.26278	-0.00100
continuation in the next page	

Table 3 – continuation

Moment, HJD-2400000	(O-C), days
55960.44078	-0.00115
55962.61903	-0.00106
55964.79718	-0.00106
55966.97532	-0.00108
55969.15349	-0.00106
55971.33167	-0.00104
55973.50978	-0.00108
55975.68789	-0.00112
55977.86600	-0.00117
55980.04415	-0.00117
55982.22232	-0.00116
55984.40043	-0.00120
55990.93486	-0.00124
55993.11305	-0.00120
55995.29120	-0.00120
55997.46934	-0.00122
55999.64750	-0.00121
56001.82566	-0.00121
56004.00383	-0.00119
56006.18199	-0.00119
56008.36016	-0.00117
56010.53822	-0.00126
56012.71645	-0.00119
56014.89457	-0.00122
56017.07265	-0.00130
56019.25077	-0.00133
56021.42895	-0.00131
56023.60710	-0.00131
56025.78530	-0.00127
56027.96348	-0.00124
56030.14168	-0.00119
56032.31980	-0.00123
56034.49793	-0.00125
56036.67620	-0.00114
56038.85433	-0.00116
56041.03247	-0.00118
56043.21064	-0.00116
56045.38880	-0.00116
56047.56695	-0.00116
56049.74509	-0.00117
56051.92322	-0.00120
56054.10136	-0.00121
continuation in the next page	

Table 3 – continuation

Moment, HJD-2400000	(O-C), days
56056.27953	-0.00120
56058.45768	-0.00120
56060.63583	-0.00121
56062.81401	-0.00118
56064.99215	-0.00119
56067.17031	-0.00119
56069.34844	-0.00121
56071.52663	-0.00118
56073.70473	-0.00123
56075.88309	-0.00103
56080.23923	-0.00120
56082.41739	-0.00119
56084.59558	-0.00115
56086.77377	-0.00112
56088.95187	-0.00117
56091.13003	-0.00117
56093.30819	-0.00116
56095.48629	-0.00122
56097.66443	-0.00123
56099.84256	-0.00126
56102.02071	-0.00126
56104.19885	-0.00127
56108.55520	-0.00123
56110.73337	-0.00122
56112.91154	-0.00120
56115.08969	-0.00121
56117.26788	-0.00117
56119.44606	-0.00114
56121.62421	-0.00115
56130.33683	-0.00115
56132.51495	-0.00118
56134.69314	-0.00115
56136.87126	-0.00118
56141.22754	-0.00121
56143.40564	-0.00126
56145.58383	-0.00123
56147.76194	-0.00127
56149.94015	-0.00122
56152.11831	-0.00121
56154.29644	-0.00124
56156.47455	-0.00128
56158.65285	-0.00113
continuation in the next page	

Table 3 – continuation

Moment, HJD-2400000	(O-C), days
56160.83101	-0.00113
56163.00918	-0.00111
56165.18734	-0.00111
56167.36547	-0.00113
56171.72170	-0.00121
56176.07805	-0.00117
56178.25616	-0.00121
56182.61266	-0.00102
56184.79079	-0.00105
56186.96889	-0.00110
56189.14696	-0.00119
56191.32514	-0.00116
56193.50333	-0.00112
56195.68142	-0.00119
56197.85966	-0.00110
56200.03782	-0.00110
56202.21585	-0.00122
56206.57218	-0.00120
56208.75036	-0.00118
56210.92850	-0.00119
56213.10672	-0.00112
56215.28484	-0.00116
56217.46300	-0.00115
56219.64117	-0.00114
56221.81930	-0.00116
56223.99745	-0.00117
56226.17558	-0.00119
56228.35372	-0.00120
56230.53189	-0.00119
56232.71004	-0.00119
56234.88821	-0.00118
56237.06636	-0.00118
56239.24460	-0.00110
56241.42268	-0.00117
56243.60089	-0.00112
56245.77903	-0.00113
56252.31344	-0.00118
56254.49160	-0.00118
56256.66976	-0.00117
56258.84793	-0.00116
56261.02618	-0.00106
56263.20430	-0.00110
continuation in the next page	

Table 3 – continuation

Moment, HJD-2400000	(O-C), days
56265.38245	-0.00110
56267.56055	-0.00115
56269.73872	-0.00114
56271.91687	-0.00114
56274.09496	-0.00121
56276.27306	-0.00126
56278.45124	-0.00124
56280.62939	-0.00124
56282.80746	-0.00132
56284.98561	-0.00133
56287.16373	-0.00136
56289.34193	-0.00132
56291.52008	-0.00132
56293.69826	-0.00130
56295.87646	-0.00125
56298.05464	-0.00123
56300.23279	-0.00123
56302.41098	-0.00119
56306.76730	-0.00118
56308.94545	-0.00119
56322.01433	-0.00123
56324.19246	-0.00126
56326.37065	-0.00122
56328.54883	-0.00120
56330.72696	-0.00122
56332.90509	-0.00125
56335.08323	-0.00126
56337.26137	-0.00127
56339.43956	-0.00124
56341.61770	-0.00125
56343.79586	-0.00125
56345.97401	-0.00125
56348.15220	-0.00122
56350.33032	-0.00125
56352.50855	-0.00118
56354.68662	-0.00126
56356.86482	-0.00121
56361.22111	-0.00123
56363.39919	-0.00131
56365.57734	-0.00131
56367.75560	-0.00121
56369.93379	-0.00117
continuation in the next page	

Table 3 – continuation

Moment, HJD-2400000	(O-C), days
56372.11196	-0.00116
56374.29005	-0.00122
56376.46825	-0.00117
56378.64637	-0.00121
56380.82450	-0.00123
56383.00266	-0.00123
56385.18082	-0.00122
56387.35900	-0.00120
56389.53716	-0.00119

Table 4: Amplitude of the theoretical curve and the orbital period of the third body obtained from a Fourier expansion using three values of the orbital period of FL Lyr

Orbital period of FL Lyr, days	Light-time effect amplitude, s	Light-time effect period, years
2.17815440	4.8	7.2
2.17815408	9.9	12.4
2.17815414	7.6	11.3

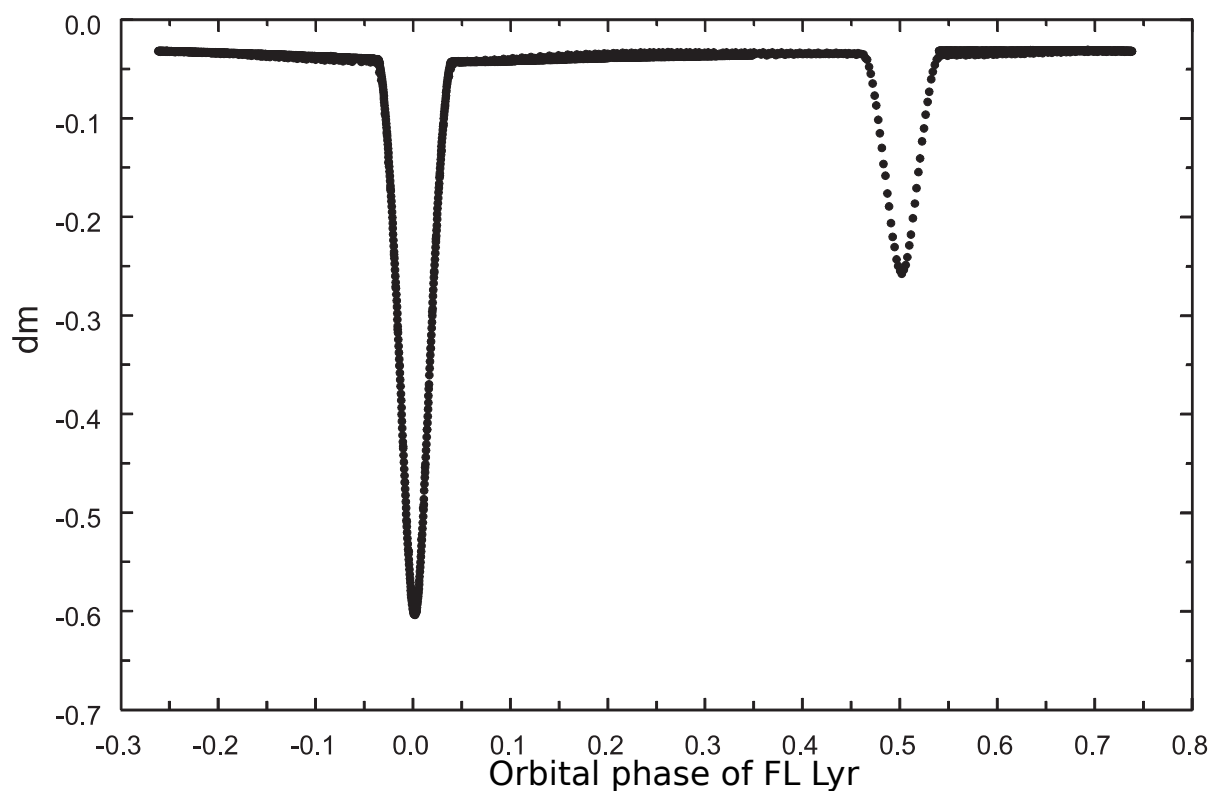


Figure 1: Light curve of FL Lyr compiled from Kepler observations between HJD 55031.54198 and HJD 55042.44777. It includes the times of primary minimum HJD 55032.54697, HJD 55034.72509, HJD 55036.90328, HJD 55039.08140, and HJD 55041.25957. All HJD times actually correspond to HJD2400000.

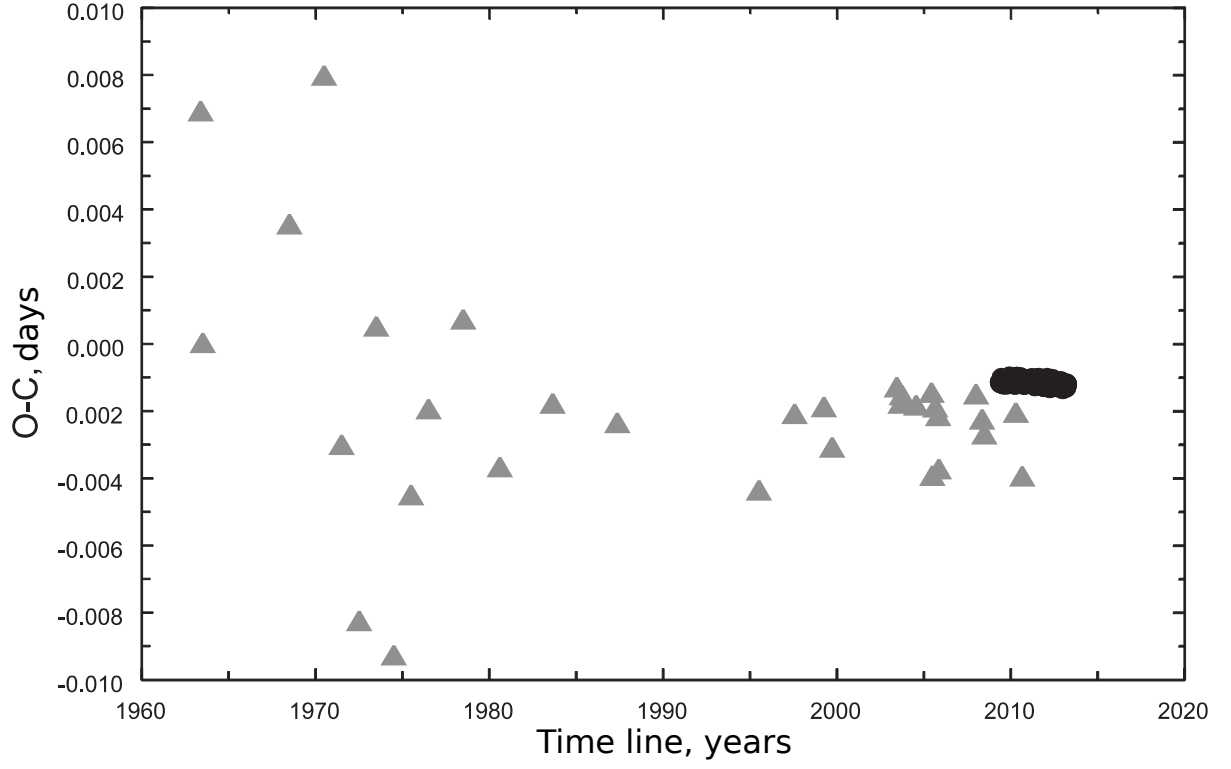


Figure 2: Times of minima of FL Lyr. The black circles show Kepler data (Table 3), and the gray triangles data from ground-based observations (Table 2). The x axis plots the dates of the observations and the y axis the differences between the observed times of minimum and times of minimum calculated using 1.

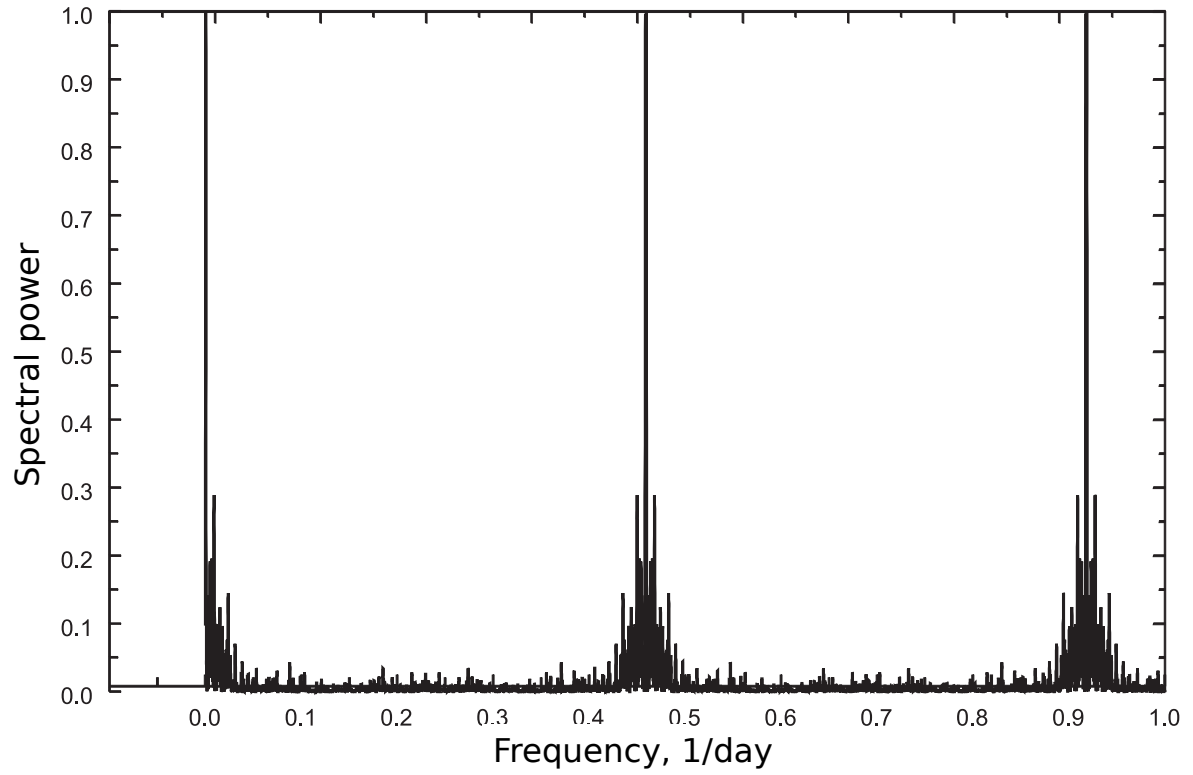


Figure 3: Power spectrum of FL Lyr in relative units calculated using the ephemeris 1.

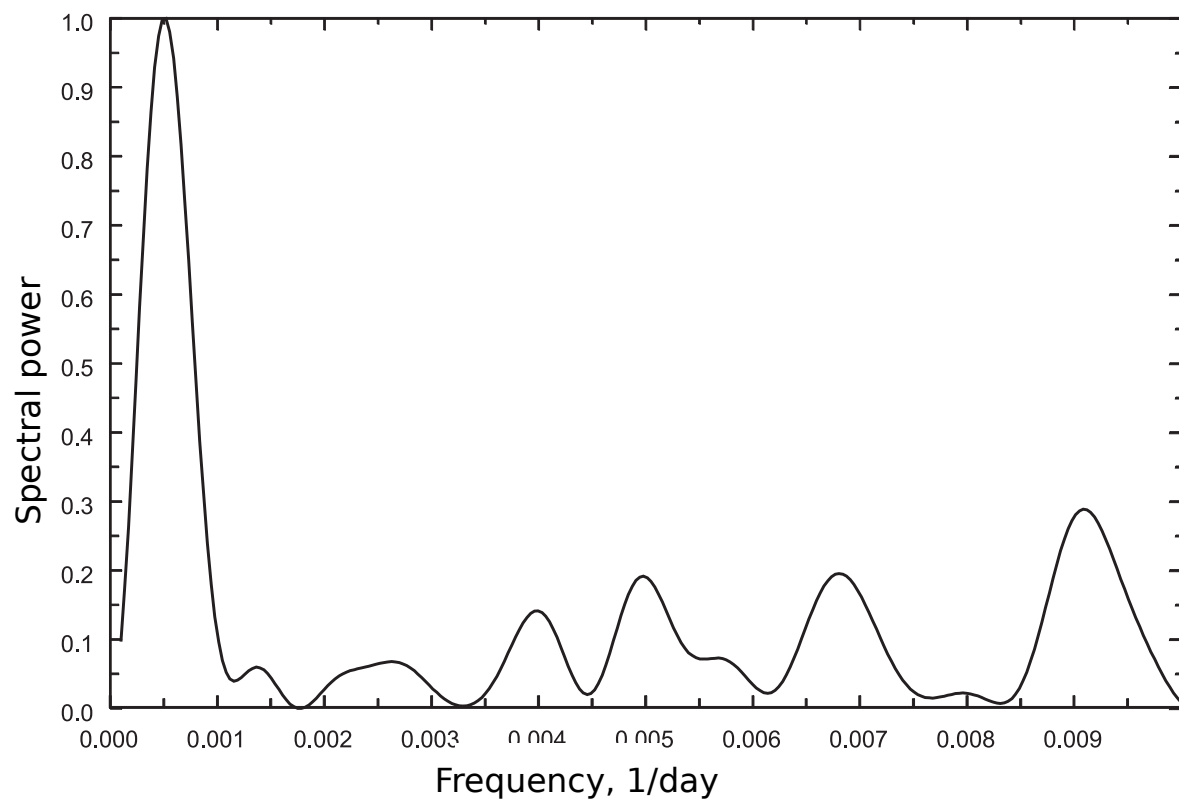


Figure 4: Same as Fig. 3 on a larger scale, for the part at low frequencies..

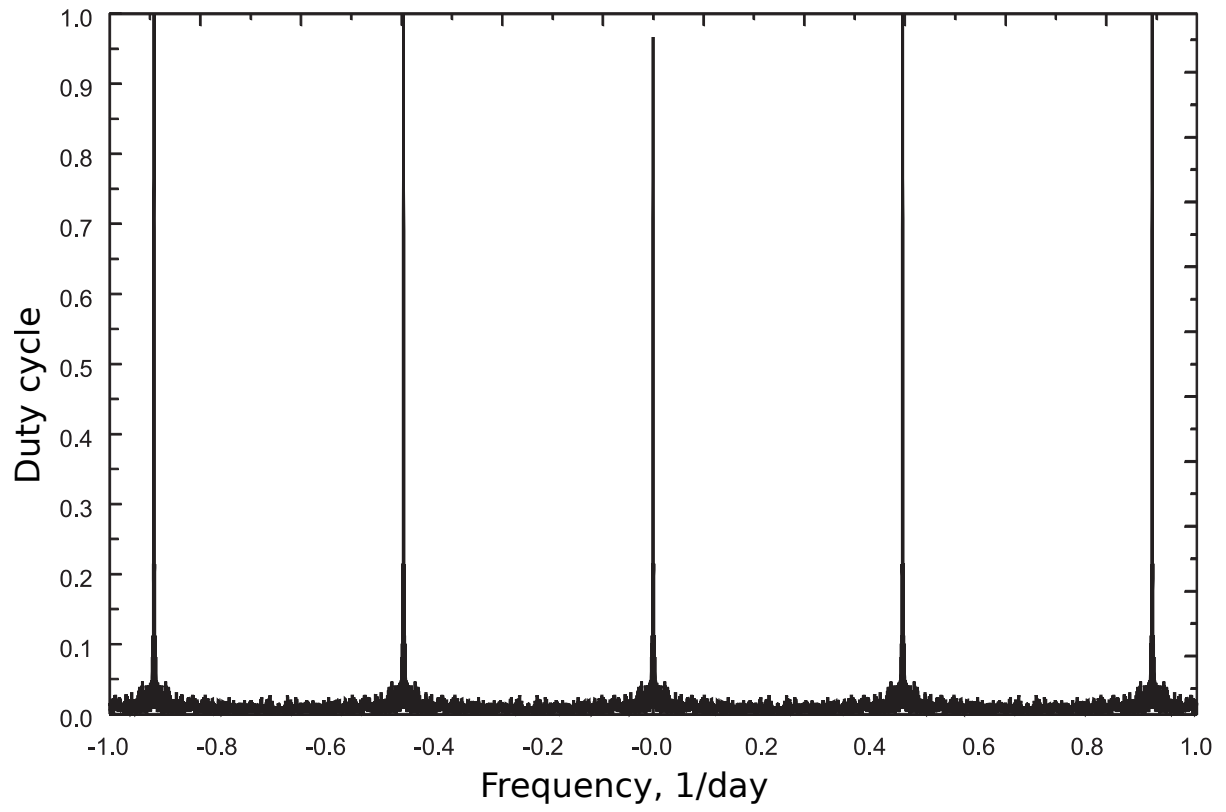


Figure 5: Duty cycle as a function of the signal frequency.

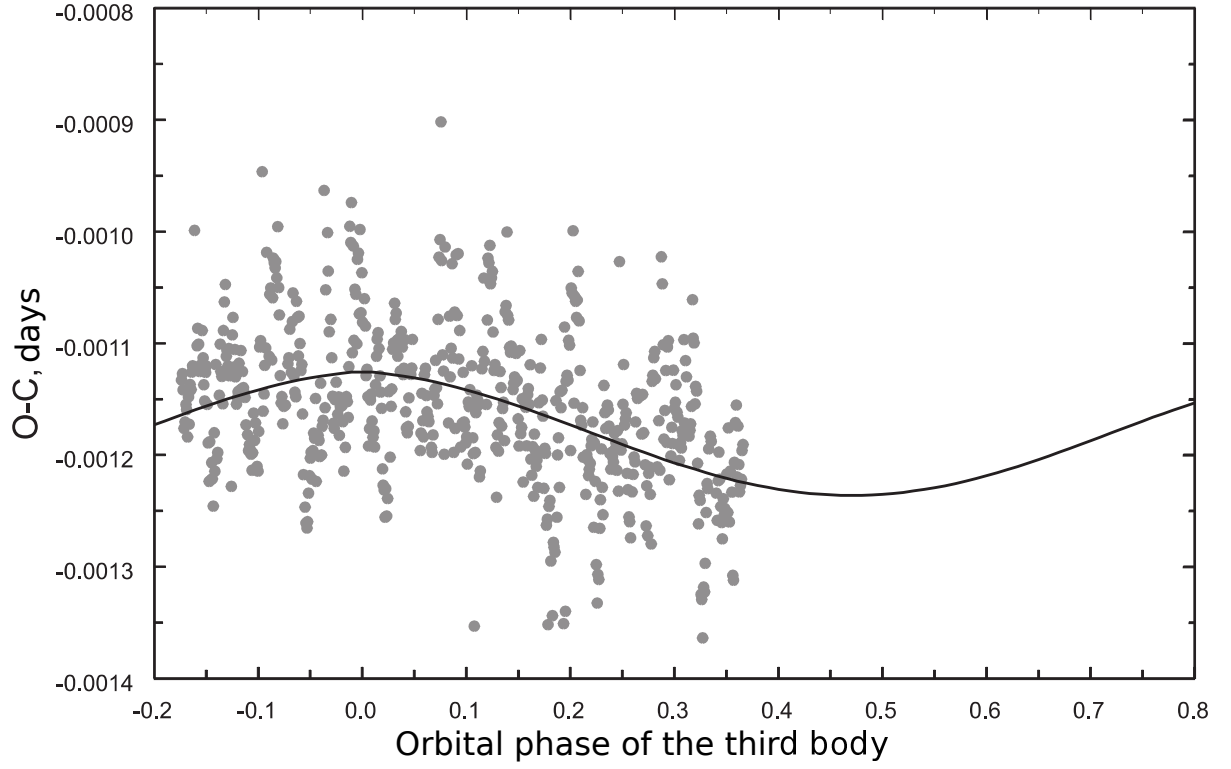


Figure 6: Light-time effect for the third body. The ephemeris 1 was used in the calculations. See Table 4 for the period and amplitude of the light-time effect. The solid curve shows the theoretical curve, and the gray circles the observations.

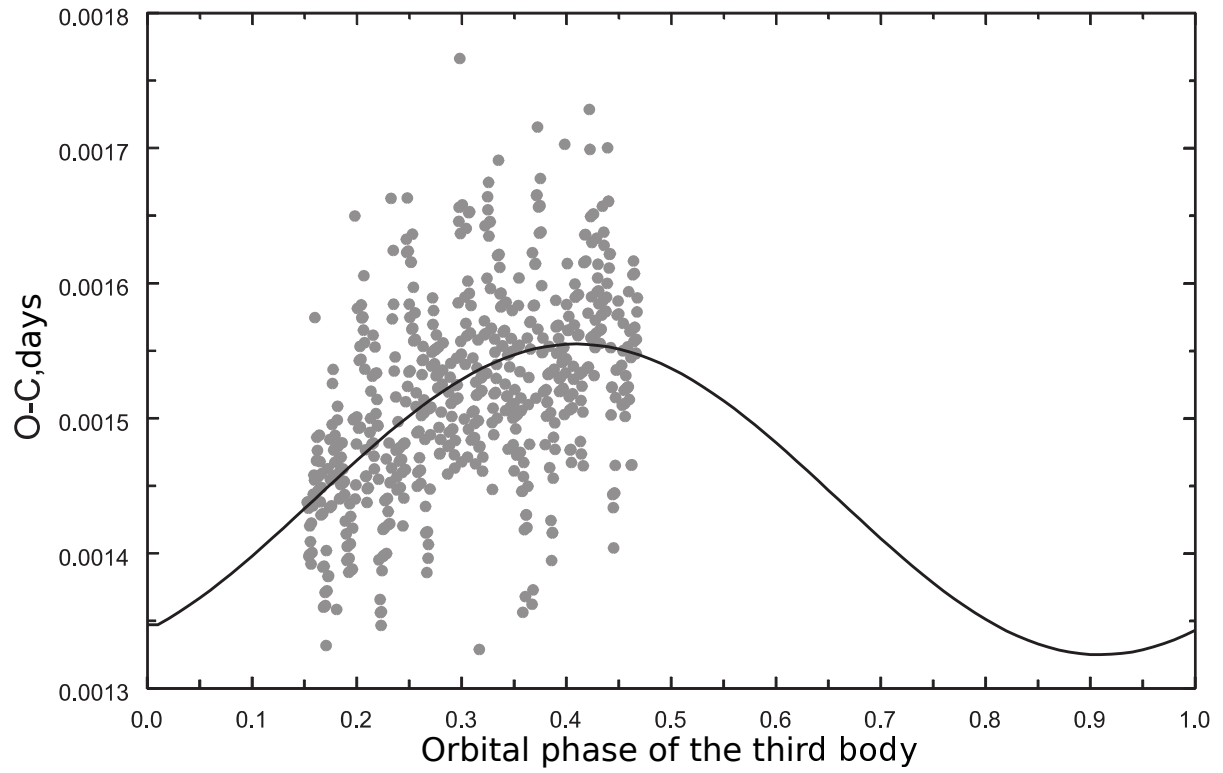


Figure 7: Same as Fig. 6 using the ephemeris 2.

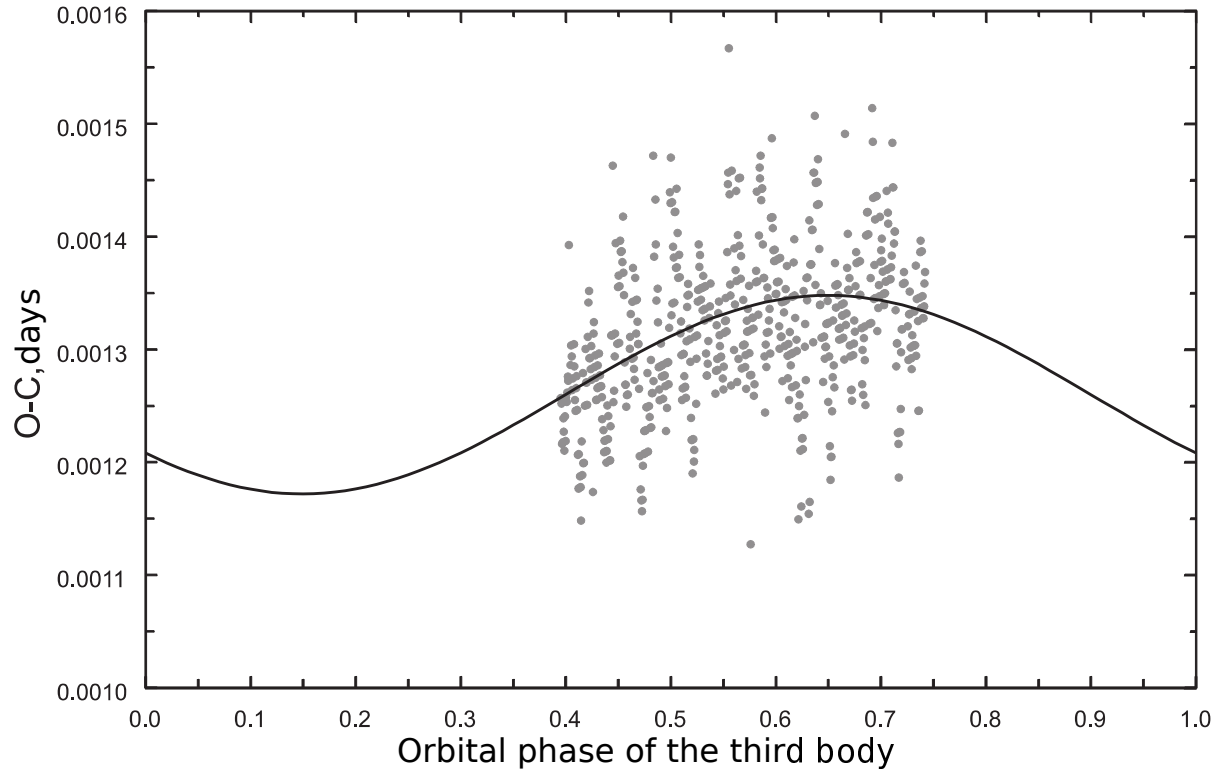


Figure 8: Same as Fig. 6 using the ephemeris 3.